

THE STUDY OF A SEASONAL SOLAR CCHP SYSTEM BASED ON EVACUATED FLAT-PLATE COLLECTORS AND ORGANIC RANKINE CYCLE

by

**Guangtao GAO^a, Jing LI^{b*}, Jingyu CAO^a, Honglun YANG^a,
Gang PEI^a, and Yuehong SU^b**

^a University of Science and Technology of China,

Department of Thermal Science and Energy Engineering, Hefei, China

^b University of Nottingham, Department of Architecture and Built Environment,
University Park, Nottingham, UK

Original scientific paper

<https://doi.org/10.2298/TSCI180804101G>

The demands of cooling, heating and electricity in residential buildings are varied with seasons. This article presented a seasonal solar combined cooling heating and power (CCHP) system based on evacuated flat-plate collectors and organic Rankine cycle. The heat collected by evacuated flat-plate collectors is used to drive the organic Rankine cycle unit in spring, autumn and winter; and drive the double-effect lithium bromide absorption chiller in summer. The organic Rankine cycle condensation heat is used to yield hot water in spring and autumn, whereas supply heating in winter. The system thermodynamic performance was analyzed. The results show that the system thermal efficiency in spring, autumn and winter, $\eta_{\text{sys},I}$ increases as organic Rankine cycle evaporation temperature, T_6 , and evacuated flat-plate collectors outlet temperature, T_2 , decrease. The maximum $\eta_{\text{sys},I}$ of 67.0% is achieved when $T_6 = 80$ °C and $T_2 = 100$ °C. In summer, the system thermal efficiency, $\eta_{\text{sys},II}$, increases first and then decreases with the increment of T_2 . The maximum $\eta_{\text{sys},II}$ of 69.9% is obtained at $T_2 = 136$ °C. The system output performance in Beijing and Lanzhou is better than that in Hefei. The average output power, heating capacity, hot water and cooling capacity are 50-72 kWh per day, 989-1514 kWh per day, 49-57 ton per day and 1812-2311 kWh per day, respectively. The system exergy efficiency increases from 17.8-40.8% after integrating the organic Rankine cycle unit.

Key words: solar CCHP system, evacuated flat-plate collector,
organic Rankine cycle, seasonal operation

Introduction

The rapidly growing world energy consumption has already raised concerns over supply difficulties, exhaustion of fossil fuels and heavy environmental impacts, such as ozone layer depletion, global warming, climate change, etc. The global contribution from buildings towards energy consumption, both residential and commercial, has reached 20-40% [1]. For example, in 2014, China's total building energy consumption was 814 million ton cool equivalent, accounting for 19.12% of the country's total energy consumption [2]. In 2016, about 40% (i. e., 39 quadrillion British thermal units) of total U. S. energy consumption was consumed by

* Corresponding author, e-mail: lijing83@ustc.edu.cn; peigang@ustc.edu.cn

the residential and commercial sectors [3]. Therefore, the use of renewable energy to provide heating, cooling and electricity for buildings can effectively alleviate the energy crisis and environment problems.

The solar thermal-driven CCHP system is attractive due to the fact that the cost-effective thermal storage unit can be integrated to guarantee the stable operation [4]. However, the common non-concentrating solar collectors (flat plate collectors, vacuum tube collectors and heat pipe collectors, *etc.*) generally operate at temperatures below 100 °C, and are not capable of driving double-effect absorption chillers [5-7]. Although concentrating solar collectors (parabolic trough collectors and linear Fresnel collectors, *etc.*) have a working temperature even above 400 °C, they cannot use diffuse solar radiation and are inconvenient to integrate with buildings due to the complex tracking equipment [8-10].

Recently, a new type of non-concentrating solar collector, evacuated flat-plate collector (EFPC), has been developed to eliminate the shortcomings of the above collectors. As shown in fig. 1, EFPC consists of glass cover, heat absorber, support pillars, back sheet and metal frame. The glass is supported by pillars passing through holes in the absorber. There is no heat conduction between the pillars and the absorber. The heat absorber integrated with fluid tubes is placed in the high-vacuum envelope. Reducing internal pressure in a solar panel envelope only slightly reduces convection until the mean-free-path of residual gas molecules gets longer than the gap between the absorber and the envelope. Under such condition (typically reached at 10^{-1} mbar for 1.0 cm gap) molecules collide with the walls more often than with each other and

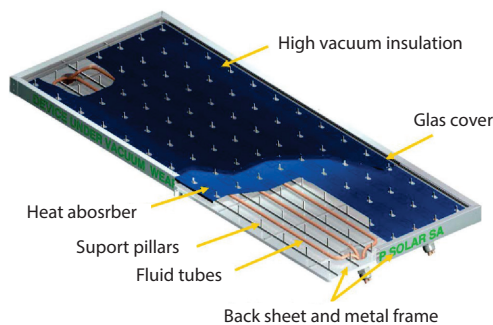


Figure 1. Structure diagram of EFPC [13]

gas heat conductivity becomes proportional to pressure and surface area only, disappearing below 10^{-3} mbar (high-vacuum) [11]. Due to the fact that the vacuum in EFPC envelope is as high as 10^{-3} - 10^{-9} mbar, the heat losses caused by convection is suppressed. The operating temperature can be guaranteed at 100-180 °C, meanwhile, the efficiency is higher than 50% [12]. Up to now, some research institutions and companies have investigated and manufactured EFPC products, such as TVP solar, SRB Energy, Genersys, CERN, *etc.* [13, 14].

On the other hand, organic Rankine cycle (ORC) is preferable to generate electricity due to its outstanding thermodynamic performance at low-medium temperature heat sources [15-17]. The condensation heat in ORC unit can be used for supplying floor radiant heating and central hot water as the required temperatures are just around 45 °C [18, 19]. It not only reduces the exergy losses, but also makes the system has flexible seasonal operating modes to adapt the various demands of cooling, heating and electricity in buildings. To date, many studies on solar ORC systems have been focused towards system structure optimization and working fluid selection [20, 21]. For example, Sonsaree *et al.*, [22] analyzed a solar ORC system with three different types of non-concentrating solar collectors, including compound parabolic concentrator, evacuated-tube and flat-plate collectors. Singh and Mishra [23] studied a solar parabolic trough collectors driven combined the topping supercritical CO₂ cycle and the bottoming ORC cycle. Habka and Ajib [24] found that mixtures perform better than the pure fluids in a solar combined heat and power unit based on ORC. Rajabloo *et al.* [25] indicated that the presence of thermal decomposition of working fluid would aggravate ORC power plant performance. However, little research has been done on the EFPC-driven solar ORC system, especially CCHP system. Kutlu *et al.* [26] investigated the

off-design performance of EFPC-ORC power system with consideration of transient behavior of the pressurized hot water storage unit, and found that power output can be adjusted by controlling the mass-flow rate of the circulation water and it is possible to meet electricity demand at night. Moss *et al.* [27] discovered that EFPC-ORC system is suitable for supplying both heat and power by comparison with conventional photovoltaic/thermal panels. Freeman *et al.* [28] studied an EFPC-driven solar ORC combined heat and power system without cooling capacity. Moreover, Calis *et al.* [29] analyzed the thermo-economic performance of EFPC-driven solar ORC combined heat and power system, and found that the system may be economically feasible for the majority of locations in the Mediterranean area (pay-back periods around 10 years). The current study proposed a seasonal solar thermal-driven CCHP system based on EFPC and ORC, and mainly analyzed the system performance in different seasons and regions.

System description

As displayed in fig. 2, the proposed CCHP system is composed of EFPC field, water storage unit, ORC unit (surrounded by red rectangle), double-effect lithium bromide (LiBr) absorption chiller (enclosed by blue rectangle), floor radiant heating unit and central hot water supply unit (connected with ORC condenser). When solar irradiation is sufficient, the EFPC collect solar energy to heat water medium, one part of which accumulates in the storage tank, and the remaining part of which enters the ORC evaporator to drive the ORC unit in spring, autumn and winter or flows into the high pressure generator to drive the double-effect LiBr absorption chiller in summer. Particularly, the ORC condensation heat is used to yield hot water in spring and autumn, whereas drive the floor radiant heating unit in winter. When solar irradiation is weak or at night, the heat stored in the storage tank is used to drive the thermal devices.

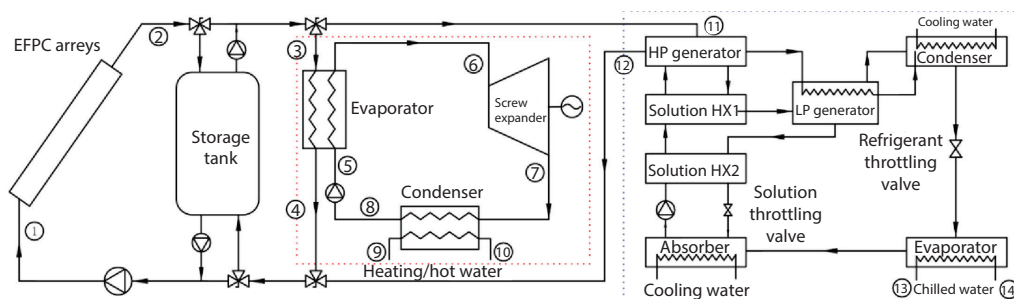


Figure 2. Schematic diagram of the proposed CCHP system; HP – high pressure, HX – heat exchanger, LP – low pressure

Mathematical model

The efficiency of solar collector is defined as the ratio of the useful thermal energy leaving the collector to the useable solar irradiance falling on the collector's aperture area. The efficiency of EFPC provided by manufacturer is expressed [30]:

$$\eta_{\text{EFPC}} = 0.759 - 0.508 \frac{T_{\text{av}} - T_a}{G} - 0.007 \frac{(T_{\text{av}} - T_a)^2}{G} \quad (1)$$

$$T_{\text{av}} = \frac{T_1 + T_2}{2} = \frac{T_3 + T_4}{2} = \frac{T_{11} + T_{12}}{2} \quad (2)$$

where T_{av} is the average temperature between EFPC filed inlet and outlet T_a – the ambient temperature, and G – the solar irradiance.

The work generated by ORC screw expander is calculated:

$$w_{SE} = \dot{m}_{ORC} (h_6 - h_7) = \dot{m}_{ORC} (h_6 - h_7) \varepsilon_{SE} \quad (3)$$

where ε_{SE} is the ORC screw expander isentropic efficiency, and ε_{SE} of 75-80% is claimed for most screw expander products.

The work required by ORC pump is determined:

$$w_p = \dot{m}_{ORC} (h_5 - h_8) = \frac{\dot{m}_{ORC} (h_{5s} - h_8)}{\varepsilon_p} \quad (4)$$

where ε_p is the ORC pump isentropic efficiency and is assumed to be 80% in this study.

The ORC thermal efficiency is expressed:

$$\eta_{ORC} = \frac{w_{net}}{q_{in,ORC}} = \frac{(w_{SE} \varepsilon_g - w_p)}{\dot{m}_{ORC} (h_6 - h_5)} = \frac{(w_{SE} \varepsilon_g - w_p)}{\dot{m}_w (h_3 - h_4)} \quad (5)$$

where ε_g is the generator efficiency and is usually up to 95%, η_{ORC} indicates how effectively the thermal energy is converted into electricity.

The ORC condensation heat used for space heating and hot water is calculated:

$$q_{hot} = \dot{m}_{w,hot} (h_{10} - h_9) = \dot{m}_{ORC} (h_7 - h_8) \quad (6)$$

In spring, autumn, and winter, the whole system thermal efficiency is determined:

$$\eta_{sys,I} = \eta_{EFPC} \frac{w_{net} + q_{hot}}{q_{in,ORC}} = \eta_{EFPC} \frac{(w_{SE} \varepsilon_g - w_p) + \dot{m}_{ORC} (h_7 - h_8)}{\dot{m}_w (h_3 - h_4)} \quad (7)$$

where $\eta_{sys,I}$ indicates the utilization efficiency of thermal energy in spring, autumn and winter, including electricity, heating and hot water supplies.

Exergy is the maximum useful work which can be extracted from a system as it reversibly comes into equilibrium with its environment. The exergy of water in EFPC or storage tank is expressed:

$$e_w = \dot{m}_w [(h_3 - T_a s_3) - (h_4 - T_a s_4)] \quad (8)$$

The exergy of hot water in ORC condenser is calculated:

$$e_{w,hot} = \dot{m}_{w,hot} [(h_{10} - T_a s_{10}) - (h_9 - T_a s_9)] \quad (9)$$

Exergy efficiency computes the effectiveness of a system relative to its performance in reversible conditions. It is defined as the ratio of the thermal efficiency of an actual system compared to an idealized or reversible version of the system. The proposed system exergy efficiency in spring, autumn and winter is determined:

$$\eta_{e,w} = \frac{e_{w,hot} + w_{net}}{e_w} = \frac{\dot{m}_{w,hot} [(h_{10} - T_a s_{10}) - (h_9 - T_a s_9)] + (w_{SE} \varepsilon_g - w_p)}{\dot{m}_w [(h_3 - T_a s_3) - (h_4 - T_a s_4)]} \quad (10)$$

The COP of refrigerating system is a ratio of useful cooling provided to work required. The COP of double-effect LiBr absorption chiller is defined:

$$COP = \frac{q_{cooling}}{q_{in,LiBr}} = \frac{\dot{m}_{w,cooling} (h_{13} - h_{14})}{\dot{m}_w (h_{11} - h_{12})} \quad (11)$$

The value of COP is related to heat source inlet temperature, and it can be calculated by [31]:

$$COP = -11.37075 + 0.28008T_{11} - 0.00235T_{11}^2 + 8.80155 \cdot 10^{-6}T_{11}^3 - 1.23616 \cdot 10^{-8}T_{11}^4 \quad (12)$$

In summer, the whole system thermal efficiency is expressed:

$$\eta_{\text{sys,II}} = \eta_{\text{EFPC}} COP \quad (13)$$

where $\eta_{\text{sys,II}}$ indicates the utilization efficiency of thermal energy in summer for cooling.

Results and discussion

In this article, R245fa is adopted as ORC working fluid. In April and October, the ORC condensation heat is used to yield hot water. In January, February, March, November, and December, the ORC condensation heat is used to drive floor radiant heating unit. In May, June, July, August and September, double-effect LiBr absorption chiller is worked. The reference solar irradiance, sunshine duration and ambient temperature for designing the system are supposed to be 800 W/m², 6 hours and 25 °C, respectively. The system seasonal performance is analyzed with typical meteorological year data in Beijing, Hefei and Lanzhou [32]. Besides, the related specific parameters are shown in tab. 1.

Table 1. Specific parameters of the system

Term	Value
ORC net output power, w_{net}	10 kW
Absorption chiller cooling power, q_{cooling}	250 kW
Screw expander isentropic efficiency, ε_{SE}	0.75
ORC pump isentropic efficiency, ε_{p}	0.80
Generator efficiency, ε_{g}	0.95
ORC condensation temperature, T_8	50 °C
Heating/hot water inlet temperature, T_9	15 °C
Heating/hot water outlet temperature, T_{10}	45 °C
Water temperature drop in HP generator, $\Delta T = T_{11} - T_{12}$	15 °C
Minimum temperature difference, ΔT_{min}	5 °C
Volume of storage tank, V_{tank}	25 m ³

Optimum working conditions

The system optimum working conditions are determined in accordance with the system thermal efficiency, $\eta_{\text{sys,I}}$ or $\eta_{\text{sys,II}}$. As shown in fig. 3(a), $\eta_{\text{sys,I}}$ increases as ORC evaporation temperature, T_6 , and EFPC outlet temperature, T_2 , decrease. The maximum $\eta_{\text{sys,I}}$ is achieved when $T_6 = 80$ °C and $T_2 = 100$ °C. It should be noted that although the ORC thermal efficiency, $\eta_{\text{sys,II}}$, can be improved at higher ORC evaporation temperature and EFPC inlet temperature, the available condensation heat, q_{hot} , is reduced, resulting in an almost constant heat utilization efficiency, $\eta_{\text{ORC}} + q_{\text{hot}}/q_{\text{in,ORC}}$. Consequently, the EFPC efficiency, η_{EFPC} , has a decisive effect on $\eta_{\text{sys,I}}$ according to eq. (7).

Besides, $\eta_{\text{sys,II}}$ increases first and then decreases with the increment of EFPC outlet temperature, as displayed in fig. 3(b). This is mainly because η_{EFPC} is deteriorated whereas the

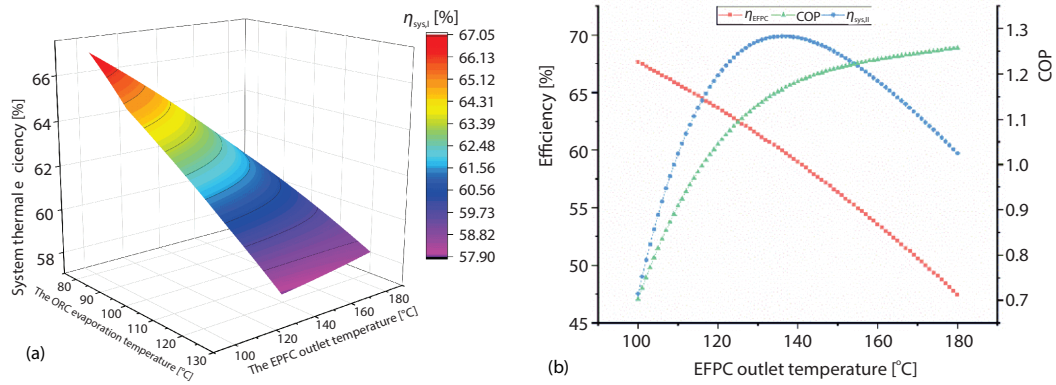


Figure 3. System thermal efficiency; (a) spring, autumn, and winter, (b) summer

COP of double-effect LiBr absorption chiller is improved as EFPC outlet temperature rises. The maximum $\eta_{\text{sys,II}}$ is obtained at $T_2 = 136 \text{ }^\circ\text{C}$, meanwhile, η_{EFPC} is 60.0% and COP is 1.17, as shown in tab. 2. In addition, it is worth noting that too high EFPC outlet temperature is not suitable in summer because the improvement of COP is limited while η_{EFPC} is significantly reduced.

Table 2. Parameters in optimum working condition

	$T_{1,\text{opt}}$ [$^\circ\text{C}$]	$T_{2,\text{opt}}$ [$^\circ\text{C}$]	\dot{m}_{ORC} [kgs^{-1}]	\dot{m}_w [kgs^{-1}]	$\dot{m}_{w,\text{hot}}$ [kgs^{-1}]	η_{EFPC} [%]	η_{ORC} [%]	COP	$\eta_{\text{sys,I}}$ [%]	$\eta_{\text{sys,II}}$ [%]
Spring Autumn Winter	80.8	100	1.24	2.99	2.73	68.0	4.1	–	67.0	–
Summer	121	136	–	3.36	–	60.0	–	1.17	–	69.9

System output performance

According to the ORC net output power, absorption chiller cooling power, and optimum working conditions, the required area of EFPC is about 595 m², of which used for normal heat collection and heat storage is, respectively, 450 m² and 145 m². The EFPC field can operate for 9 hours in the daytime, from 8:00 a. m. to 5:00 p. m. After that, the heat stored in tank can be used to drive the ORC or the absorption chiller to work normally for 0.88-2.32 hours, as shown in tab. 3.

Table 3. Runtime of ORC unit and absorption chiller using storage heat, unit: hour

Region	ORC unit							Absorption chiller				
	Jan.	Feb.	Mar.	Apr.	Oct.	Nov.	Dec.	May	June	July	Aug.	Sept.
Beijing	1.48	1.68	1.97	2.28	1.90	1.48	1.44	2.27	2.19	1.84	1.80	2.10
Lanzhou	1.47	1.66	1.86	2.29	2.12	1.88	1.49	2.27	2.17	2.31	2.32	2.19
Hefei	0.88	1.02	1.31	1.78	1.50	1.25	1.01	1.79	1.87	1.92	1.76	1.49

The system output performance in different seasons and areas is presented in fig. 4. The portion containing fill pattern represents the system output generated from the stored thermal energy. Compared with that in Beijing and Lanzhou, the system annual output performance is worst in Hefei due to the lowest EFPC efficiency. Specifically, the average η_{EFPC} in Hefei is about 50.8% during the normal operation period, whereas it is around 52.0% and 54.6% in Beijing and Lanzhou, respectively. This is mainly because the solar irradiance is weak in Hefei. The average annual solar irradiance is 563551 W/m² and 463 W/m² in Beijing, Lanzhou and Hefei, respectively.

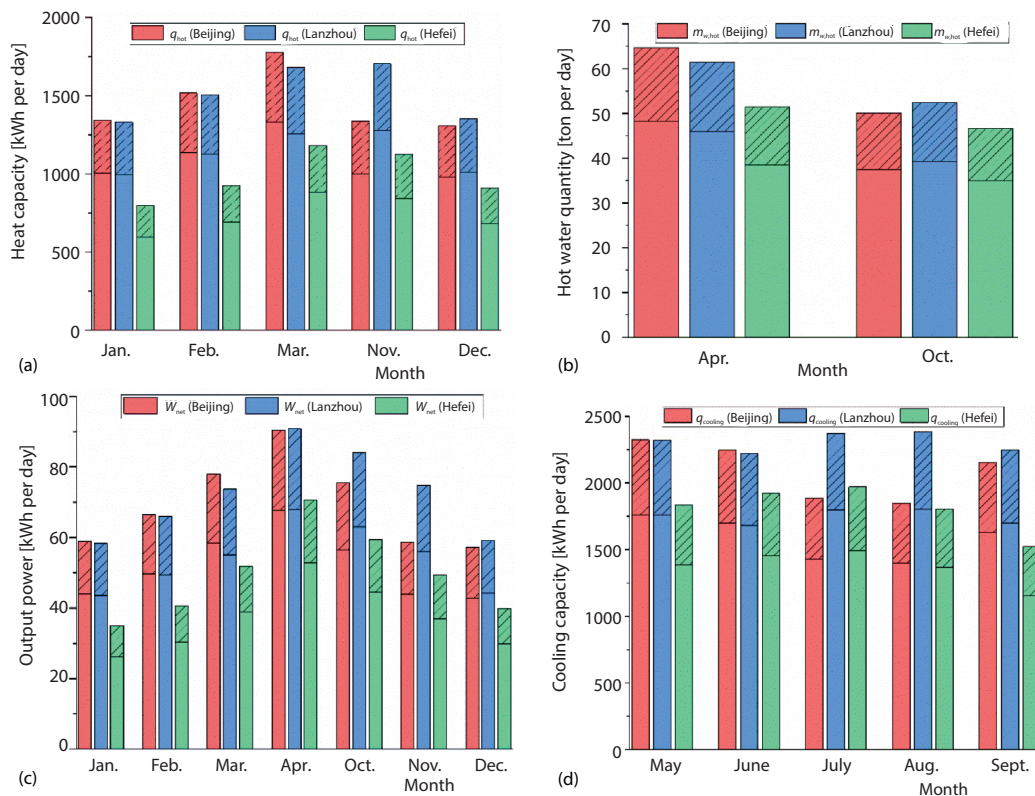


Figure 4. System output performance in different seasons; (a) heating capacity; (b) hot water quantity, (c) output power, and (d) cooling capacity

In spring, autumn, and winter, the ORC unit can guarantee an average output power of 69 kWh per day, 72 kWh per day, and 50 kWh per day in Beijing, Lanzhou and Hefei, respectively. Correspondingly, an average heating capacity of 1457 kWh per day, 1514 kWh per day, and 989 kWh per day is available in winter; and an average hot water quantity of 57 ton per day, 57 ton per day, and 49 ton per day is obtainable in spring and autumn. For double-effect LiBr absorption chiller, it can provide an average cooling capacity of 2091 kWh per day, 2311 kWh per day, and 1812 kWh per day in Beijing, Lanzhou and Hefei during summer. Assuming that the building's energy consumption standards are, respectively 2 kWh person per day of electricity, 80 W/m² of heating, 60 L person per day of hot water and 100 W/m² of cooling [33-35], the system can meet the energy demands of such buildings and residents, as shown in tab. 4. It is worth noting that the generated hot water can be used by at least 800 people, far exceeding

the number of residents consuming electricity. In order to obtain higher electrical power, it is advisable to decrease ORC condensation temperature after producing sufficient hot water in spring and autumn.

Table 4. The scale of residential area supplied by the system

Region	Building area, [m ²]		Number of residents, person	
	Heating	Cooling	Electricity	Hot water
Beijing	1713	1892	34	956
Lanzhou	1770	2053	36	949
Hefei	1222	1681	24	817

Comparison with the cogeneration system without ORC

Assuming that the heat collected by EFPC field is used directly for supplying heating and hot water, then the exergy utilization efficiency, $e_{w,hot}/e_w$, in optimum working conditions is only about 17.8%. Specifically, the exergy of water in EFPC or storage tank, $e_w = 43.5$ kW, the exergy of available hot water, $e_w = 7.7$ kW. This is mainly because the temperature difference between the water in EFPC field and floor radiant heating unit as well as central hot water supply unit is higher than 50 °C, resulting in huge exergy losses. Comparably, the system exergy efficiency, $\eta_{e,w}$, can rise to 40.8% after integrating the ORC unit because a part of the available exergy is converted into electricity. Obviously, the proposed system can realize the cascade utilization of the collected energy in spring, autumn and winter and is therefore, more efficient.

Conclusions

This paper presented a seasonal solar-driven CCHP system based on EFPC and ORC, and mainly analyzed the system thermodynamic performance in different seasons and areas. The results show that.

- The system thermal efficiency in spring, autumn and winter, $\eta_{sys,I}$, increases as ORC evaporation temperature, T_6 , and EFPC outlet temperature, T_2 , decrease. The maximum $\eta_{sys,I}$ of 67.0% is achieved when $T_6 = 80$ °C and $T_2 = 100$ °C. Besides, the system thermal efficiency in summer, $\eta_{sys,I}$, increases first and then decreases with the increment of T_2 . The maximum $\eta_{sys,I}$ of 69.9% is obtained at $T_2 = 136$ °C.
- The average EFPC efficiency is higher than 50.8% when operation temperature is above 100 °C. The required area of EFPC is about 595 m², of which used for heat storage is 145 m².
- The system output performance in Beijing and Lanzhou is better than that in Hefei. The average output power, heating capacity, hot water and cooling capacity are 50-72 kWh per day, 989-1514 kWh per day, 49-57 ton per day and 1812-2311 kWh per day, respectively.
- The system exergy efficiency is about 17.8% assuming that the heat collected by EFPC field is used directly for supplying heating and hot water, while increases to 40.8% after integrating the ORC unit.

Future work

In the following year, a demonstration system will be built in the west campus at the University of Science and Technology of China. On this basis, the system annual performance will be studied through experiments.

Acknowledgment

The study was sponsored by the National Science Foundation of China (NSFC 51476159, 51761145109, and 51776193), EU Marie Curie International Incoming Fellowships Program (703746) and International Technology Cooperation Program of the Anhui Province of China (BJ2090130038).

Nomenclature

e – exergy, [kW]
 G – solar irradiance, [Wm^{-2}]
 h – enthalpy, [kW]
 m – mass, [ton]
 \dot{m} – mass-flow rate, [kgs^{-1}]
 q – heat or cooling power, [kW]
 s – entropy, [$\text{kJkg}^{-1}\text{k}^{-1}$]
 T – temperature, [$^{\circ}\text{C}$]
 V – volume, [m^3]
 w – work, [kW]
 ΔT – temperature difference, [$^{\circ}\text{C}$]

Greek symbols

ε – isentropic efficiency
 η – thermal efficiency, [%]

Subscri

a – ambient
av – average

g – generator
I – operating mode in spring, autumn and winter
II – operating mode in summer
min – minimum
opt – optimal
P – pump
s – isentropic
SE – screw expander
sys – system
tank – storage tank
w – water

Acronyms

CCHP – combined cooling, heating and power
EFPC – evacuated flat-plate collector
LiBr – lithium bromide
ORC – organic Rankine cycle

References

- [1] Perez-Lombard, L., et al., A Review on Buildings Energy Consumption Information, *Energy and Buildings*, 40 (2008), 3, pp. 394-398
- [2] ***, The Report of China-building Energy Consumption, CABEE, <http://www.efchina.org/Attachments/Report/report-20170710-1/report-20170710-1>
- [3] ***, How Much Energy is Consumed in U. S. Residential and Commercial Buildings, U. S. Energy Information Administration, <https://www.eia.gov/tools/faqs/faq.php?id=86&t=1>
- [4] Modi, A., et al., A Review of Solar Energy Based Heat and Power Generation Systems, *Renewable and Sustainable Energy Reviews*, 67 (2017), Jan., pp. 1047-1064
- [5] Jafarkazemi, F., et al., Energy and Exergy Efficiency of Heat Pipe Evacuated Tube Solar Collectors, *Thermal Science*, 20 (2016), 1, pp. 327-335
- [6] Oko, C. O. C., Nnamchi, S. N., Heat Transfer in a Low Latitude Flat-Plate Solar Collector, *Thermal Science*, 16 (2012), 2, pp. 583-591
- [7] Mahesh, A., Solar Collectors and Adsorption Materials Aspects of Cooling System, *Renewable and Sustainable Energy Reviews*, 73 (2017), June, pp. 1300-1312
- [8] Lazzarin, R. M., Noro, M., Past, Present, Future of Solar Cooling: Technical and Economical Considerations, *Solar Energy*, 172 (2018), Part 1, pp. 2-13
- [9] Senthil, R., Cheralathan, M., Effect of Non-Uniform Temperature Distribution on Surface Absorption Receiver in Parabolic Dish Solar Concentrator, *Thermal Science*, 21 (2017), 5, pp. 2011-2019
- [10] Karimi Sadaghiyani, O., et al., Two New Designs of Parabolic Solar Collectors, *Thermal Science*, 18 (2014), 2, pp. 323-334
- [11] ***, TVP Solar SA, Thermal Vacuum Power Charged™ Technology, 2017
- [12] ***, MT-Power Datasheet, TVP Solar SA, [http://www.tvpsolar.com/files/pagine/1508933997_MT-Power%20Datasheet%20\(v4%20SK\).pdf](http://www.tvpsolar.com/files/pagine/1508933997_MT-Power%20Datasheet%20(v4%20SK).pdf)
- [13] ***, Evacuated Flat-Plate Collector, TVP Solar SA, <http://www.tvpsolar.com/products.html>
- [14] ***, Vacuum Flat Collector, Genersys, <http://www.thermosolar.com/english/Solar.html>

- [15] Li, J., Structural Optimization and Experimental Investigation of the Organic Rankine Cycle for Solar Thermal Power Generation, Ph. D. thesis, University of Science and Technology of China, Hefei, China, 2015
- [16] Macchi, E., Astolfi, M., *Organic Rankine Cycle (ORC) Power Systems, Technologies and Applications*, Woodhead Publishing, Sawston, UK, 2017
- [17] Boydak, O., *et al.*, Thermodynamic Investigation of Organic Rankine Cycle Energy Recovery System and Recent Studies, *Thermal Science*, 22 (2018), 6, pp. 2679-2690
- [18] ***, Industry Standard of People's Republic of China, Technical Specification for Floor Radiant Heating, JGJ142-2004, 2004
- [19] ***, National Standard of the People's Republic of China, Code for Design of Building Water Supply and Drainage, GB 50015-2003, 2003
- [20] Barbazza, L., *et al.*, Optimal Design of Compact Organic Rankine Cycle Units for Domestic Solar Applications, *Thermal Science*, 18 (2014), 3, pp. 811-822
- [21] Zhu, Q. D., *et al.*, Performance Analysis of Organic Rankine Cycles Using Different Working Fluids, *Thermal Science*, 19 (2015), 1, pp. 179-191
- [22] Sonsaree, S., *et al.*, A Small-Scale Solar Organic Rankine Cycle Power Plant in Thailand: Three Types of Non-Concentrating Solar Collectors, *Solar Energy*, 162 (2018), Mar., pp. 541-560
- [23] Singh, H., Mishra, R. S., Performance Analysis of Solar Parabolic trough Collectors Driven Combined Supercritical CO₂ and Organic Rankine Cycle, Engineering Science and Technology, *International Journal*, 21 (2018), 3, pp. 451-464
- [24] Habka, M., Ajib, S., Performance Estimation of Mixtures in Solar Organic Rankine Cycle with Two Mini Cogeneration Options for Improvement Purpose, *Sustainable Energy Technologies and Assessments*, 16 (2016), Aug., pp. 174-189
- [25] Rajabloo, T., *et al.*, Effect of a Partial Thermal Decomposition of the Working Fluid on the Performances of ORC Power Plants, *Energy*, 133 (2017), Aug., pp. 1013-1026
- [26] Kutlu, C., *et al.*, Off-Design Performance Modelling of a Solar Organic Rankine Cycle Integrated with Pressurized Hot Water Storage Unit for Community Level Application, *Energy Conversion and Management*, 166 (2018), June, pp. 132-145
- [27] Moss, R. W., *et al.*, Performance and Operational Effectiveness of Evacuated Flat Plate Solar Collectors Compared with Conventional Thermal, PVT and PV Panels, *Applied Energy*, 216 (2018), Apr., pp. 588-601
- [28] Freeman, J., *et al.*, An Assessment of Solar-Powered Organic Rankine Cycle Systems for Combined Heating and Power in UK Domestic Applications, *Applied Energy*, 138 (2015), Jan., pp. 605-620
- [29] Calise, F., *et al.*, Design and Simulation of a Prototype of a Small-Scale Solar CHP System Based on Evacuated Flat-Plate Solar Collectors and Organic Rankine Cycle, *Energy Conversion and Management*, 90 (2015), Jan., pp. 347-363
- [30] ***, MT-Power v3.11, TVP Solar SA, Durability, Reliability and Thermal Performance of A Solar Collector, Solar KeyMark Certificate, 11COL1028, 2012
- [31] Han, C. W., The Performance Analysis of Solar Double-effect Lithium Bromide Absorption Refrigeration System, Report, University of Science and Technology of China, 2009
- [32] ***, Typical Meteorological Year Data in Hefei, Energyplus, <https://energyplus.net/weather>
- [33] ***, National Standard of the People's Republic of China, Steam and Hot Water Type Lithium Bromide Absorption Water Chiller, GB/T 18431-2001, 2001
- [34] ***, The Electricity Consumption of Chinese Residents, National Bureau of Statistics of China, <http://www.stats.gov.cn/english/>
- [35] ***, National Standard of the People's Republic of China, Code for Urban Heating Supply Planning, GB/T 51074-2015, 2015